

#### Contents lists available at ScienceDirect

# Talanta

journal homepage: www.elsevier.com/locate/talanta



# Elemental imaging of heterogeneous inorganic archaeological samples by means of simultaneous laser induced breakdown spectroscopy and laser ablation inductively coupled plasma mass spectrometry measurements



Olga Syta<sup>a</sup>, Barbara Wagner<sup>a,\*</sup>, Ewa Bulska<sup>a</sup>, Dobrochna Zielińska<sup>b</sup>, Grażyna Zofia Żukowska<sup>c</sup>, Jhanis Gonzalez<sup>d,e</sup>, Richard Russo<sup>d,e</sup>

- <sup>a</sup> Faculty of Chemistry, Biological and Chemical Research Centre, University of Warsaw, Warsaw, Poland
- <sup>b</sup> Institute of Archaeology, Faculty of History, University of Warsaw, Warsaw, Poland
- <sup>c</sup> Chemical Faculty, Warsaw University of Technology, Warsaw, Poland
- <sup>d</sup> Lawrence Berkeley National Laboratory, University of California, Berkeley, CA, USA
- e Applied Spectra, Inc., Fremont, CA, USA

#### ARTICLE INFO

## Keywords: LA-ICP-MS LIBS Imaging Pigment identification

#### ABSTRACT

Multilayered fragments of murals were used to evaluate the usefulness of two laser-based instrumental methods: laser induced breakdown spectroscopy (LIBS) and laser ablation (LA) inductively coupled plasma mass spectrometry (ICP-MS) for elemental imaging of unique historic samples. Simultaneous LA/LIBS measurements with the use of 266 nm Nd:YAG laser were performed on cross-sections of mediaeval Nubian objects with specific blue painting layers including either Egyptian blue (CaCuSi $_4$ O $_1$ O) or lapis lazuli (Na $_{8-10}$ Al $_6$ Si $_6$ O $_2$ 4S $_{2-4}$ ). A combined use of both laser-based methods allowed for clear distinguishing of blue pigments based on visual imaging of a chemical composition of heterogeneous archaeological inorganic samples. The identification of the pigments was confirmed with Raman spectroscopy.

# 1. Introduction

Laser ablation inductively coupled plasma mass spectrometry (LA-ICP-MS) and laser induced breakdown spectroscopy (LIBS) are widely applied in different scientific disciplines [1-4]. The role of LA-ICP-MS in elemental distribution analysis is constantly increasing, and has resulted in particularly large progress for bioimaging [5]. Achievement of the highest possible resolution is one of the main goals of LA-ICP-MS applications in this field due to trace concentrations of investigated elements and small dimensions of samples subjected to MSI (mass spectrometry imaging) e.g. single cells or kidney tubules [6]. Biological samples represent soft, relatively homogenous organic matrix with physicochemical properties of the matrices that vary slightly. Heterogeneous mixtures of various minerals are characterized by far greater density differences, hardness, transparency and melting temperature [7]. It can be difficult to achieve the successful optimization of operating conditions while laser based instrumental methods are used for imaging [8]. A legible interpretation of the registered LA-ICP-MS data may be hampered if the ablation threshold could not be exceeded for all components of analyzed samples but a plasma plume generated at the surface might allow for excitation of atoms and emission of characteristic lines for each present element.

Multilayered cross-sections of wall paintings can be regarded as good examples of such heterogeneous and complex objects. A crosssection is a minuscule fragment detached from the artefact to observe and analyze all layers of it. Usually a material for preparation of the cross-section is sampled with a surgical knife, then fixed and embedded in a colorless resin. One edge of the cross-section is cut smoothly, ground and polished in order to give a plane surface for the detailed microscopic observation. The pioneer of preparation of paint crosssections was Laurie [9] who described the procedure in 1914. Although some changes have been introduced since that time, the main idea of the proposed cross-sectioning has not changed significantly [10]. Wax initially used as the mounting media was changed by different types of synthetic resins: epoxy, acrylic, polyester or others [11]. Analysis of cross-sections provides large amount of precise morphological and compositional information about each layer of the investigated object. Color, shape and size of pigment particles, their texture as well as layer thickness can be superimposed with chemical analysis of pigments and binding media. Performing tests, which might be inadvisable or dangerous for the whole object itself, can be done in a micro-scale keeping the popularity of cross-sectioning at the high level [12].

E-mail address: barbog@chem.uw.edu.pl (B. Wagner).

<sup>\*</sup> Corresponding author.

One of the most popular methods applied for investigations of cross-sections taken from oil paintings is SEM-EDS [13–15]; elemental mapping of such samples has been also performed by LA-ICP-MS [16]. In this work Panighello et al. [16] discussed a probable provenance of smalt (CoO.nSiO<sub>2</sub>) from 17th century Dutch paintings. Layers of oil paintings were mapped in details by laser ablation ICP-MS measurements showing the potential of using LA-ICP-MS for multilayered cross-sections of precious artifacts.

LIBS was also applied in spatial analysis of unique historic objects [17–20]. In the work of Lopez et al. [17] fluctuations in Ca to Fe ratio allowed for distinguishing between glaze coating and ceramic bulk of Roman pottery. Depth profiling for reconstruction of stratigraphy of oil [18] and wall-paintings [19,20] was done during spot micro-sampling followed by registration of signal intensities of selected emission lines during subsequent laser shots performed on the same area. Macroscopic and microscopic composition of wall-paintings was more highly heterogeneous with painting layers on plasters rich in mineralogical inclusions characterized by various physicochemical properties [21].

Either LIBS or LA-ICP-MS were used in these works individually or were supported by a molecular method [22–24]. Meissner et al. [25] was the first who showed that LIBS can be used as a method complementary to LA-ICP-MS. Since 2004 a few articles concerning the use of LIBS and LA-ICP-MS together have been published [26–30] focusing on advantages of each method. Low limits of detection in a sub-ppb range were listed as the important advantage of LA-ICP-MS measurements while possibility to determine elements like H, N, O, Si, Se, As or S was underlined as the domain of LIBS [31]. These two spectroscopic methods can be regarded complementary in providing information about all elements on the periodic chart and extending the dynamic range from trace to major elements [31–33] as well as collecting of all elemental information from the same sample location.

The consistency of the data obtained from independent analyses could vary significantly due to challenging cross-correlation between: (i) selected sample areas, (ii) spatial and depth resolution, and (iii) excitation volumes, especially in the case of the analysis of heterogeneous samples [34]. Simultaneous LA/LIBS elemental mapping of relatively homogeneous magnesium based alloys [35], soft biological tissues [36] or imaging of hard mineral [37] were already described. Cross sections of multilayered historic wall-paintings represent mixtures of very heterogeneous composition possibly including grains of hard minerals, particles of pigments, lime, gypsum and binding media therefore it was interesting to evaluate the usefulness of simultaneous LA-LIBS measurements of such complex matrix.

# 1.1. Aim of the work

Studies of historical objects require careful consideration of material taken from artifacts, and often refer to chemical data collected by means of various instrumental methods from one sample. This work was devoted to simultaneous elemental imaging of heterogeneous mineral samples by means of LA-ICP-MS/LIBS and focused on identification of the chemical composition of paintings layers. Samples of mediaeval Nubian (modern Sudan) wall paintings were selected to represent variable elemental composition of materials with a special attention devoted to the composition of blue pigments. Concordance of the results obtained by means of LA-ICP-MS and LIBS during laser interaction with heterogeneous inorganic archaeological samples was checked.

# 2. Material and methods

# 2.1. Samples

6 tiny multilayered fragments were studied. They represent 7th–14th century wall-paintings from three archaeological sites (Fig. 1) and consist of different number of layers with variable degree of inhomogeneity. Samples (Fig. 2), prepared in the form of cross-sections,

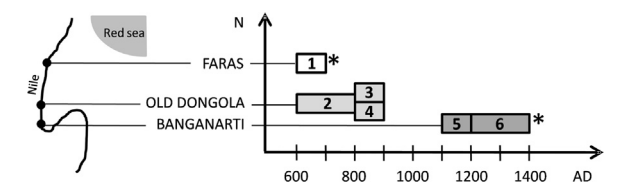


**Fig. 1.** A diagram showing the historic context of the samples (numbered from 1 to 6). N – north direction, indicates the relative location of the excavation sites; AD- Anno Domini, indicates the dating of the buildings, which the samples were taken from. Asterisks point out the samples which were selected as the exemplary cross-sections for elemental imaging.

were embedded in acrylic resin VillacrylS/0 (Zhermack Technical, Italy), ground flat with corundum papers and polished with fine diamond pastes (down to the final diameter of 0.5 mm for the diamond powder). All layers of the murals (painting layers, whitewash and plaster) were visible in the cross-sections with the thickness ranging from 8  $\mu$ m to 100  $\mu$ m. Samples were numbered from 1 to 6. The sample\_1 was selected together with the sample\_6 as the exemplary cross-sections for elemental imaging due to the highest discrepancies between them in age, geographical distance as well as their macroscopic morphology and structure of painting layers.

Two blue pigments were expected in the samples: either the extremely expensive, natural mineral lapis lazuli  $(Na_{8-10}Al_6Si_6O_{24}S_{2-4})$  or artificially prepared, relatively popular and easily accessible Egyptian blue  $(CaCuSi_4O_{10})$  [38]. Due to differences in their price and availability, these pigments can be assumed as indicators of wealth and importance of monuments from which they were taken.

## 2.2. Reference materials

SRM NIST 610 (National Institute of Standards and Technology) was used to check daily the instrumental performance for operating stability together with SRM NIST 679 (brick clay). SRM NIST 679 was selected as the matrix-matched material and used as the external standard. It was palletized before measurements. A hydraulic press, with the pressure of 5 t was used to obtain a stable, solid form of the reference material.

Certified values of the elemental composition of NIST 679 referred to GeoReM (georem.mpch-mainz.gwdg.de). Limits of detection (Table 1) were calculated based on the measurements of NIST 679 according to the formula:

LOD = blank + 3\*SD,

where: *blank* - average signal intensity registered for each element before ablation started, *SD* – standard deviation of the calculated blank.

For LIBS detection limits were calculated using emission line wavelengths given in Table 2. The limit of detection for Cu is given here as the informative value only, indicating that it is above the certified Cu content in the SRM NIST 679.

## 2.3. Instrumentation

## 2.3.1. Elemental imaging

Elemental imaging was performed with the use of a J200 tandem LA/LIBS instrument (Applied Spectra Inc., Fremont, CA) equipped with a 266 nm Nd:YAG laser and a six channel spectrometer with CCD detection covering a spectral range from 180 to 1050 nm. The J200 system was connected to an Aurora Elite mass spectrometer (Bruker, USA). The respective instrumental parameters were selected after careful optimization of laser parameters for tandem LA/LIBS measurements (Table 3). The laser energy output was kept at the level high enough to form the plasma on the surface of the sample for efficient LIBS measurements, but it was also maintained at the level sufficiently low to keep the sample possibly untouched for the entire time of investigations.













Fig. 2. Microscopic images of the samples 1–6. Asterisks point out the samples which were selected as the exemplary cross-sections for elemental imaging (Fig. 4) due to the highest discrepancies between them in age, geographical distance, morphology and painting layer.

Table 1 Comparison of LODs  $[\mu g/g]$  obtained during LA/LIBS imaging of selected elements calculated based on SRM NIST 679 measurements.

	LIBS	LA-ICP-MS
Na	7.0	244.8
Mg	4.8	7.7
Al	13.5	0.0(1)
Si	40.3	1124.2
K	8.7	13.5
Ca	11.1	314.5
Ti	3.4	3.8
Mn	10.0	0.9
Fe	33.5	28.1
Cu	> 28.4ª	4.5
Sr	0.4	0.0(1)
Ва	0.7	0.4

<sup>&</sup>lt;sup>a</sup> Cu was not detected in NIST 679 by means of LIBS, therefore LOD for Cu using LIBS was only estimated as the value higher than Cu content in the SRM.

Two groups of elements (Table 2) were selected relatively to their importance for the chemical identification of archaeological materials composition. The elevated content of Ca, Cu, Si, O, Na, Al or S can be linked to the presence of the expected pigments, while P can be detected if animal glue was used as a binder. Apart from painting layers also the composition of mineral support might include Ca, C, S, O, H, Mg, Al, Si or Fe with variable proportion. Additional monitoring of minor and trace elements can allow for distinguishing between different layers of cross-sections.

Transient signals were recorded during multi-line ablation of the cross-sections. Time delay (5 s) between ablation of two lines allowed for clear distinguishing of the data collected for each line. Blank signals were registered within the first 30 s of each measurement before the start of ablation. The raw signals were background corrected for each isotope/emission line individually. Spikes (defined as a single data point exceeding the intensities of the neighboring data for more than 2 times) were inserted by the average of two neighboring signals intensity. All maps of elemental distribution were created using Microsoft

Table 3
Optimized measurements conditions.

Laser ablation	J200 Tandem LA/LIBS				
Wavelength, nm	266				
Energy per pulse, mJ	2.5				
Beam diameter, µm	80				
Pulse repetition rate, Hz	10				
Scan rate, µm/s	10				
Multiple line, n	11				
Distance between lines, µm	20				
Area subjected to mapping, µm	$1080 \times 745$				
Time for blank registration, s	30				
ICP-MS	Aurora Elite				
RF power, W	1400				
Carrier gas flow, L/min	0.7 (He)				
Scanning mode	Peak hopping				
Dwell time per isotope, ms	5				
Sweeps	1				
Readings	4601				
Replicates	1				
Optical spectrometer system	Six channel-CCD				
Gate delay, μs	0.3				

Excel with the normalization to 1 procedure. No quantitative imaging was proposed, but a relative distribution of the selected elements over the investigated area is presented. The resolution of the maps obtained by LA-ICP-MS and LIBS is different due to discrepant number of individual data registered for each line by means of either mass (325 readings) or optical (745 readings) spectrometer.

The elemental compositions of painting layers from **samples\_3-6** were quantified with the use of NIST SRM 679 as the external standard. Si was selected as the internal standard and normalization procedure to 100 wt% was applied. The recalculations based on three selected data points from each cross-section: maximum intensity of Na signals with two neighboring data points were used for a rough calculation of the elemental composition of the pigments (Table 4).

 Table 2

 Isotopes/emission lines observed during LA-ICP-MS/LIBS measurements and used to inspect elemental distribution of the selected elements.

major elements			minor and trace elements								
isotopic mass [u]		λ [nm]	isotopic mas	s [u]	λ[nm]	isotopic mass [u]		λ [nm]			
			В	11	_	Y	89	_			
Н	-	656.3	C1	35	-	Zr	90	-			
С	12	247.9	K	39	766.5	Ag	109	-			
O	_	777.4	Sc	45	364.3	Cd	111	_			
Na	23	589.0	Ti	49	334.9	Sn	118	326.2			
Mg	26	383.8	V	51	318.7	Sb	121	237.3			
Al	27	309.3	Cr	53	427.5	Ba	137	493.4			
Si	29	288.1	Mn	55	403.1	La	139	-			
P	31	_	Co	59	_	Ce	140	_			
S	33	_	Ni	60	_	Dy	161	344.1			
Ca	43	616.2	Zn	66	_	Hf	178	_			
Fe	57	373.5	As	75	_	Hg	202	_			
Cu	65	327.4	Rb	85	_	Th	232	_			
Pb	207	-	Sr	88	460.7	U	238	-			

Table 4
Content of selected trace elements in samples\_3-6, calculated for the maximum Na signal intensities in each cross-section.

			sample_3		sample_4		sample_5		sample_6	
		LOD	cont.	SD	cont.	SD	cont.	SD	cont.	SD
wt%	Na <sub>2</sub> O	0.033	14.7	1.3	9.40	0.33	7.89	0.20	8.37	0.67
	MgO	0.001	16.3	1.5	4.25	0.14	18.8	0.2	7.35	0.07
	$Al_2O_3$	0.001	14.5	0.4	25.6	2.5	8.63	1.23	9.91	0.84
	$SiO_2$	0.236	30.7	2.0	44.9	2.0	23.9	1.0	20.8	0.5
	CaO	0.044	8.95	0.7	5.45	0.51	19.5	0.6	21.9	1.6
	P	0.020	0.08	0.01	0.29	0.06	1.85	0.18	5.03	0.18
	K	0.001	1.77	0.05	1.98	0.11	0.78	0.02	0.66	0.06
	Fe	0.003	0.75	0.07	1.40	0.14	1.63	0.10	1.09	0.08
μg/g	Ti	3.8	895	35	5669	1009	1238	180	2006	467
	V	0.3	38	2	165	10	102	10	91	6
	Cr	2.2	17	3	69	3	30	4	45	2
	As	0.1	4	0.2	1	0.3	4	0.8	21	2
	Rb	0.8	33	1	43	7	17	2	13	2
	Sr	0.0(1)	2282	194	929	114	4000	168	1780	56
	Zr	0.0(1)	29	1	113	4	67	3	40	2
	Ba	0.4	1292	204	765	90	1346	31	1398	27
	Pb	0.4	234	18	108	8	3375	46	981	36

#### 2.3.2. Raman analysis

To confirm final pigment identification Raman spectra were collected with the use of Dispersive Raman Spectrometer Nicolet Almega equipped with Olympus confocal microscope. Various excitation lines (780 or 532 nm) were used depending on the sample properties. The power of the laser was reduced to 25–50% in order to avoid sample overheating. The spectral resolution of the registered signals was about  $2~{\rm cm}^{-1}$ .

## 3. Results and discussion

## 3.1. LIBS imaging

The most suitable emission lines for LIBS elemental distribution imaging were selected after considering possible interferences. Special attention was given to Ca which could be the main element of pigment layers (Egyptian blue,  $CaCuSi_4O_{10}$ ) and mural plasters (gypsum,  $CaSO_4\cdot 2H_2O$ ) of the same samples. According to the literature usually two or more lines: Ca II 315.9 and 317.9 nm [37,39]; Ca II 393.4, 396.9 nm, Ca I 422.7 and 445.5 nm [18,40] or Ca I 428.3, 428.9, 429.8, 430.2, 430.7 and 435.5 nm [20] were used to cross-verify the distribution of Ca in the investigated samples, but sometimes only one line, e.g. Ca I 585.7 nm [22] was monitored.

In this study 8 potential Ca emission lines were discussed for eventual interferences (Fig. 3). Previous studies of Nubian murals cross-sections [41] revealed the presence of mud plaster mainly composed of Ca with quartz ( $SiO_2$ ) and Fe, Cr, Ti, V, Co, Sn inclusions. Based on the information about elemental composition of the plaster the 558.9 nm wavelength line was excluded due to possible interferences of Ca by Sn or V while the 643.9 nm wavelength was excluded as eventual presence of Fe might be expected. LIBS imaging of Ca distribution over the

defined area resulted in similar spatial information regardless of the selected emission line and were compared to the <sup>43</sup>Ca distribution map created based on LA-ICP-MS data. Finally 616.2 nm was selected as the most suitable emission line for the simultaneous LA/LIBS imaging.

## 3.2. The use of LA/LIBS tandem system

Samples 1 and 6 were selected as the exemplary cross-sections with the most divergent morphology and historic context (Fig. 1) to illustrate the effect of elemental LA/LIBS imaging. The selected elements, which are shown in Fig. 4 (O, Na, Al, Si, S, Ca and Cu) could be used as potential markers for identification of either Egyptian blue (CaCuSi<sub>4</sub>O<sub>10</sub>) or lapis lazuli (Na $_{8-10}$ Al $_6$ Si $_6$ O $_{24}$ S $_{2-4}$ ). Na and Cu are applied for identification of blue pigments by micro-chemical reactions in the classical approach [42]. The use of LA/LIBS allowed not only for detection but also for mapping of all elements over cross-sections with low limits of detection. Some of these elements (O and Si) can be found in the both pigments, and in the plaster either as quartz grains or aluminosilicates. The assignment of O, Si as well as Al to a certain layer of wall-paintings can be difficult. The presence of aluminosilicates in the mineral support of the analyzed heterogeneous samples additionally weakened the use of these elements as the lapis lazuli indicator. The use of gypsum (Ca-SO<sub>4</sub>·2H<sub>2</sub>O) in the plaster layer of sample 1 and in the whitewash of sample 6 led to exclusion of Ca and S from the list. Finally Na was selected as the marker of lapis lazuli and Cu as the marker of Egyptian blue in accordance with the classical approach [42].

LIBS and LA-ICP-MS measurements led to discrepant information about C distribution in cross-sections (Fig. 4A-B). High content of C in acrylic resin  $(C_4H_6O_2)_n$  was determined by means of LA-ICP-MS, while LIBS revealed its predominant presence in a whitewash layer (CaCO<sub>3</sub>). The reason of different carbon imaging might be explained by variable phenomenon exploited by each method based on either ablation, atomization and ionization of the analyzed material during LA-ICP-MS or plasma formation and excitation of atoms present in the sample during LIBS measurements.

The higher sensitivity of LIBS measurements was beneficial for a better definition of Si-enriched areas in all samples. The distribution of Si was correlated with Al indicating the presence of aluminosilicates, while additional detection of O allowed for detection of spatial co-location of Si and O in the plasters. Based on LA-ICP-MS investigations the presence of quartz (SiO<sub>2</sub>) in the samples could be only assumed. Co-distribution of Si and O were confirmed by LIBS and the identification of SiO<sub>2</sub> was affirmed by Raman data (128, 205, 264, 355, 402, 465 cm $^{-1}$ ). Relatively high transparency and hardness (7 in Mohs scale) of this mineral would demand higher laser energy density to achieve the effective ablation as for the other inorganic constituents of the heterogeneous cross-sections.

LIBS allowed for Na measurements with the noticeably lower limit of detection (Table 1) and the higher sensitivity than LA-ICP-MS in all samples. Imaging data collected by means of LA-ICP-MS (Fig. 4) revealed the elevated signal intensities registered for Na only in a dark blue painting layer of the **sample\_6**. The presence of Cu detected by means of LIBS was linked solely to **sample\_1** indicating the presence of

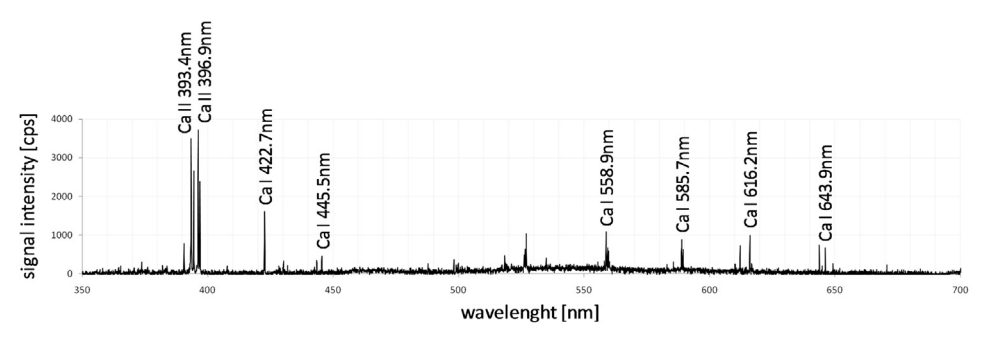
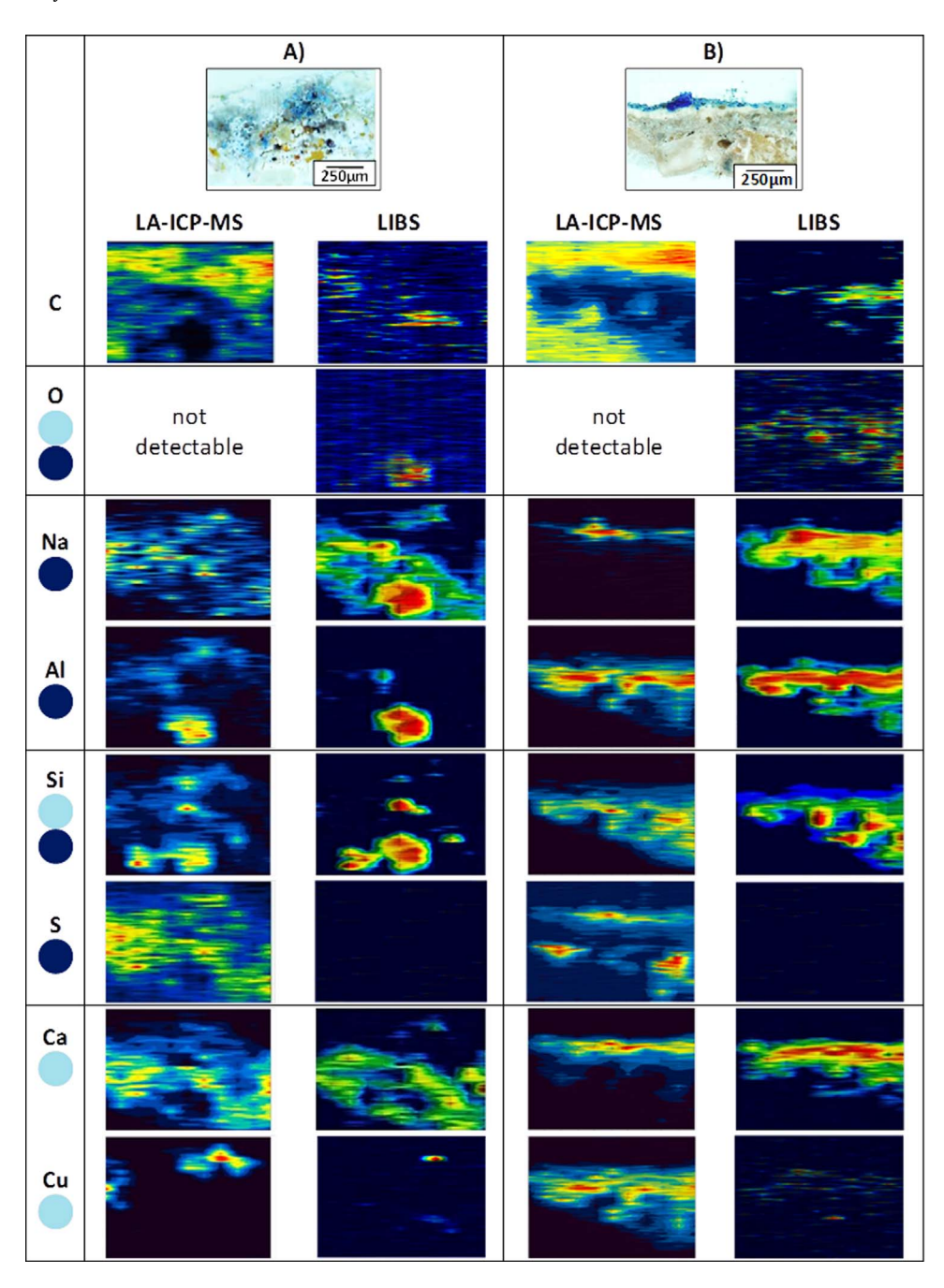


**Fig. 3.** Representative LIBS spectrum with marked Ca emission lines.



a Cu-rich mineral with the content of this element above the limit of detection of LIBS (28.4  $\mu g/g).$ 

# 3.3. Identification of blue pigments

The signal intensities registered during LA/LIBS measurements were normalized therefore only the relative distribution of Na and Cu could be observed in Fig. 5. Differences in variable minerals density, color and other physic-chemical characteristics are also reflected in fluctuations of the signal intensities, therefore the resulted information is very complex. Comparison of chemical heterogeneity of the cross-sections facilitated identification of blue pigments: Egyptian blue (CaCuSi $_4O_{10}$ ) and lapis lazuli (Na $_{8-10}Al_6Si_6O_{24}S_{2-4}$ ) based on LA-ICP-MS results for Na and LIBS data about Cu distribution.

For all samples maps of Cu distribution were created based on the signals registered during LA-ICP-MS measurements while only the areas

with the highest Cu content were detected by LIBS (Fig. 5). The Cuenriched areas could be correlated with the presence of a tiny blue grain in <code>sample\_1</code> or the blue painting layer in <code>sample\_2</code>. Contrary to Cu, a heterogeneous Na distribution with the highest Na intensities of signals registered for the plaster below the painting layer was observed in these samples. Na was clearly accumulated in the painting layers of <code>samples\_3-6</code> for which LIBS detection limit was too high to collect analytical information about Cu.

A combined use of both laser-based methods allowed for clear distinguishing of either Egyptian blue or lapis lazuli based on elemental imaging of heterogeneous archaeological inorganic samples. The identification of Egyptian blue in the grains of pigment (c.a. 20 µm) from sample\_1 and painting layer in sample\_2 was confirmed by Raman spectroscopy (Fig. 6A). Raman spectra collected from the selected areas of samples\_3-6 allowed also for identification of lapis lazuli (Fig. 6B).

Element		N	a	Cu			
Meth	nod	LA-ICP-MS	LIBS	LA-ICP-MS	LIBS		
	sample_1				• •		
	sample_2						
•	sample_3						
•	sample_4						
•	sample_5		TAKE THE	Mag.			
•	sample_6	•			1		

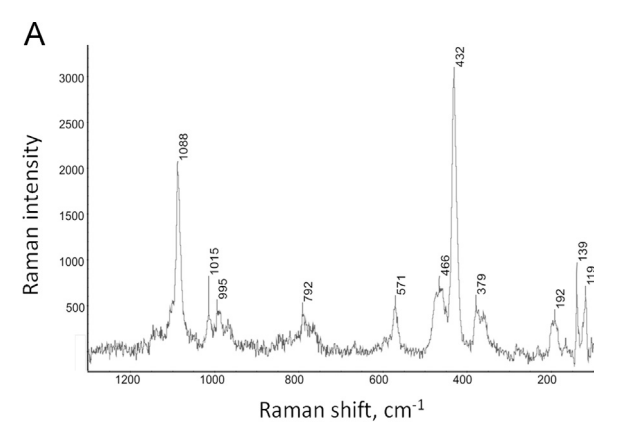
Fig. 5. Imaging data collected during LA/LIBS tandem measurements of samples\_1-6. Blue circles indicate the identification of either  $\bullet$  Egyptian blue (CaCuSi<sub>4</sub>O<sub>10</sub>) or  $\bullet$  lapis lazuli (Na<sub>8-10</sub>Al<sub>6</sub>Si<sub>6</sub>O<sub>24</sub>S<sub>2-4</sub>) in the sample. Scale of all maps is given in a.u. (0

## 3.4. LA-ICP-MS trace analysis

Egyptian blue is known as the first artificially synthesized blue pigment [38] while lapis lazuli (ultramarine) can be identified in artifacts as a pigment of either artificial or natural origin. It was the most expensive pigment and the best known provenance pointed at Afghanistan as the source of mining the mineral, although the possibility for provenancing of lapis lazuli pigment is still discussed in the literature [43]. Raw mineral with Sr and Ba might be mined in Siberia, eventual presence of As can indicate Pamir provenance [43], while Ti, V, Cr, Zr impurities support the theory about Afghan origin [44]. According to

the literature all these hypotheses would need more systematic investigations.

In this work the attempt was done only for a rough estimation of the elemental composition of lapis lazuli from the painting layers. The attention was focused on the selected elements because the detection of Ti, V, Cr, As, Rb, Sr, Zr, Ba or Pb might be helpful for distinguishing of the pigment origin (Table 4). Although solely estimation of the quantitative elemental information about the pigments could be approached, some similarities of chemical composition can be observed. Sample\_3 is similar to samples\_5-6 in respect to the high Sr and Ba content while sample\_4 is characterized by the highest Ti and V content. The



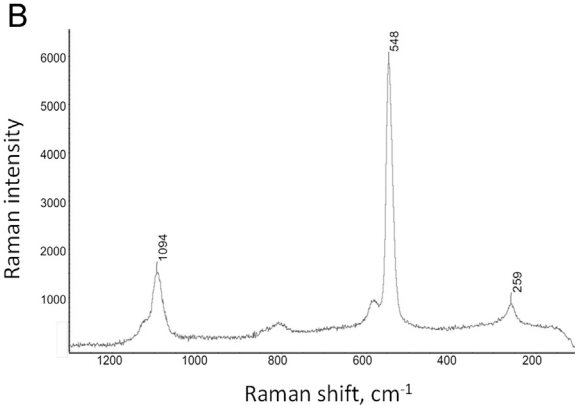


Fig. 6. Raman spectra collected from the painting layers including particles of: A) Egyptian blue and B) lapis lazuli.

presented results do not allow for solving the mystery of origin of the pigments and the provenance of lapis lazuli in Nubian wall-painting is still enigmatic.

# 4. Conclusions

LIBS and LA-ICP-MS were used for simultaneous imaging of heterogeneous inorganic archaeological samples with a special attention paid to possibility for pigment identification based on the selected markers (Cu and Na) for Egyptian blue (CaCuSi $_4O_{10}$ ) and lapis lazuli (Na $_{8-10}Al_6Si_6O_{24}S_{2-4}$ ). Elemental maps created during the measurements were coherent for most of investigated elements while the variable results of C visualization were explained by different physical processes used for LA-ICP-MS (ablation) and LIBS (excitation) performance.

The degree of sample destruction during LA/LIBS measurements was higher comparing to standalone LA-ICP-MS analysis. The importance of this feature increases when consecutive analyses are planned for the same sample like the use of Raman spectroscopy for cross-validation of the proposed identification in this work.

Egyptian blue was identified in the samples from Faras Cathedral and Cruciform Building in Old Dongola, while lapis lazuli was present in the samples from Upper Church in Banganarti, Pillar Church and Building V from Old Dongola. Apart from different location the samples were dated to the various periods (7th and 8th vs 9th–14th century) allowing archaeologists to get a new insight into the technical aspects of wall-painting in medieval kingdoms of Nubia in different periods of their history. Identification of the most precious pigment (lapis lazuli) in artworks from Banganarti and Old Dongola, led to disprove the hypothesis about the poor level of Nubian workshops.

## Acknowledgements

This work was partially realized at the Biological and Chemical Research Centre, University of Warsaw, established within the project co-financed by the European Union—European Regional Development Fund under the Operational Programme Innovative Economy (2007–2013). D.Z. would kindly acknowledge the financial support from the National Science Centre (NCN) of Poland, project No. 2011/01/D/HS3/0611.

## References

- D.W. Hahn, N. Omenetto, Laser-induced breakdown spectroscopy (LIBS), Part II: review of instrumental and methodological approaches to material analysis and applications to different fields, Appl. Spectrosc. 66 (2012) 347–419, http://dx.doi. org/10.1366/11-06574.
- [2] G. Galbacs, A critical review of recent progress in analytical laser-induced breakdown spectroscopy, Anal. Bioanal. Chem. 407 (2015) 7537–7562, http://dx.doi. org/10.1007/s00216-015-8855-3.
- [3] A. Limbeck, P. Galler, M. Bonta, G. Bauer, W. Nischkauer, F. Vanhaecke, Recent advances in quantitative LA-ICP-MS analysis: challenges and solutions in the life sciences and environmental chemistry, Anal. Bioanal. Chem. 407 (2015) 6593–6617. http://dx.doi.org/10.1007/s00216-015-8858-0.
- [4] F. Alamilla Orellana, C. Gonzalez Galvez, M. Torre Roldan, C. Garcia-Ruiz, Applications of laser-ablation-inductively-coupled plasma-mass-spectrometry in chemical analysis of forensic evidence, Trends Anal. Chem. 42 (2013) 1–34, http:// dx.doi.org/10.1016/j.trac.2012.09.015.
- [5] J.S. Becker, Imaging of metals in biological tissue by laser ablation inductively coupled plasma mass spectrometry (LA-ICP-MS): state of the art and future developments, J. Mass Spectrom. 48 (2013) 255–268, http://dx.doi.org/10.1002/jms. 3168.
- [6] J.S. Becker, A. Matusch, B. Wu, Bioimaging mass spectrometry of trace elements recent advance and applications of LA-ICP-MS: a review, Anal. Chim. Acta 835 (2014) 1–18, http://dx.doi.org/10.1016/j.aca.2014.04.048.
- [7] A. Neubeck, M. Tulej, M. Ivarsson, C. Broman, A. Riedo, S. McMahon, P. Wurz, S. Bengtson, Mineralogical determination in situ of a highly heterogeneous material using a miniaturized laser ablation mass spectrometer with high spatial resolution, Int. J. Astrobiol. 15 (2016) 133–146, http://dx.doi.org/10.1017/ S1473550415000269.
- [8] K. Novotny, J. Kaiser, M. Galiova, V. Konecna, J. Novotny, R. Malina, M. Liska, V. Kanicky, V. Otruba, Mapping of different structures on large area of granite sample using laser-ablation based analytical techniques, an exploratory study, Spectrochim. Acta, Part B 63 (2008) 1139–1144, http://dx.doi.org/10.1016/j.sab. 2008.06.011.
- [9] A.P. Laurie, The Pigments and Mediums of the Old Masters: With a Special Chapter on Microphotographic Study of Brushwork, Macmillian and Co, London, 1914.
- [10] J. Plesters, Cross-sections and chemical analysis of paint samples, Stud. Conserv. 2 (1956) 110–157, http://dx.doi.org/10.1179/sic.1956.015.
- [11] M. Derrick, L. Souza, T. Kieslich, H. Florsheim, D. Stulik, Embedding paint cross-section samples in polyester resins: problems and solutions, J. Am. Inst. Conserv. 33 (1994) 227–245, http://dx.doi.org/10.2307/3179635.
- [12] M. Gambino, F. Cappitelli, C. Catto, A. Carpen, P. Principi, L. Ghezzi, I. Bonaduce, E. Galano, P. Pucci, L. Birolo, F. Villa, F. Forlani, A simple and reliable methodology to detect egg white in art samples, J. Biosci. 38 (2013) 397–408, http://dx.doi.org/ 10.1007/s12038-013-9321-z.
- [13] C. Ricci, I. Borgia, B.G. Brunetti, C. Miliani, A. Sgamellotti, C. Seccaroni, P. Passalacqua, The Perugino's palette: integration of an extended in situ XRF study by Raman spectroscopy, J. Raman Spectrosc. 35 (2004) 616–621, http://dx.doi. org/10.1002/jrs.1131.
- [14] D. Lau, C. Villis, S. Furman, M. Livett, Multispectral and hyperspectral image analysis of elemental and micro-Raman maps of cross-sections from a 16th century painting, Anal. Chim. Acta 610 (2008) 15–24, http://dx.doi.org/10.1016/j.aca. 2007.12.043.
- [15] L. Vanco, M. Kadlecikova, J. Breza, L. Caplovic, M. Gregor, Examining the ground layer of St. Anthony from Padua 19th century oil painting by Raman spectroscopy, scanning electron microscopy and X-ray diffraction, Appl. Surf. Sc. 264 (2013) 692–698, http://dx.doi.org/10.1016/j.apsusc.2012.10.099.
- [16] S. Panighello, A. Kavcic, K. Vogel-Mikus, N.H. Nennent, A. Wellert, S.B. Hocevar, J.T. van Elteren, Investigation of smalt in cross-sections of 17th century paintings using elemental mapping by laser ablation ICP-MS, Microchem. J. 125 (2016) 105–115, http://dx.doi.org/10.1016/j.microc.2015.11.015.
- [17] A.J. Lopez, G. Nicolas, M.P. Mateo, V. Pinon, M.J. Tobar, A. Ramil, Compositional analysis of Hispanic Terra Sigillata by laser-induced breakdown spectroscopy, Spectrochim. Acta B 60 (2005) 1149–1154, http://dx.doi.org/10.1016/j.sab.2005. 05 009
- [18] E.A. Kaszewska, M. Sylwestrzak, J. Marczak, W. Skrzeczanowski, M. Iwanicka, E. Szmit-Naud, D. Anglos, P. Targowski, Depth-resolved multilayer pigment identification in paintings: combined use of laser-induced breakdown spectroscopy (LIBS) and optical coherence tomography (OCT), Appl. Spectrosc. 67 (2013) 960–972, http://dx.doi.org/10.1366/12-06703.
- [19] I. Borgia, L.M.F. Burgio, M. Corsi, R. Fantoni, V. Palleschi, A. Salvetti, M.C. Squarcialupi, E. Tognoni, Self-calibrated quantitative elemental analysis by

- laser-induced plasma spectroscopy: application to pigment analysis, J. Cult. Herit. 1 (2000) 281–286, http://dx.doi.org/10.1016/S1296-2074(00)00174-6.
- [20] M.F. Alberghina, R. Barraco, M. Brai, D. Fontana, L. Tranchina, LIBS and XRF analysis for a stratigraphic study of pictorial multilayer surfaces, Period. Mineral. 84 (2015) 569–589, http://dx.doi.org/10.2451/2015PM0024.
- [21] M. Singh, B.R. Arbad, Characterization of 4-5<sup>th</sup> century A.D. earthen plaster support layers of Ajanta mural paintings, J. Constr. Build. Mat. 82 (2015) 142–154, http:// dx.doi.org/10.1016/j.conbuildmat.2015.02.043.
- [22] Y. Lu, Y. Li, Y. Wang, S. Wang, Z. Bao, R. Zheng, Micro spatial analysis of seashell surface using laser-induced breakdown spectroscopy and Raman spectroscopy, Spectrochim. Acta B 110 (2015) 63–69, http://dx.doi.org/10.1016/j.sab.2015.05.
- [23] L. Rampazzi, B. Rizzo, C. Colombo, C. Conti, M. Realini, U. Bartolucci, M.P. Colombini, A. Spiriti, L. Facchin, The stucco decorations from St. Lorenzo in Laino (Como, Italy): the materials and the techniques employed by the "Magistri Comacini", Anal. Chim. Acta 630 (2008) 91–100, http://dx.doi.org/10.1016/j.aca. 2008.09.052
- [24] C.L. King, N. Tayles, K.C. Gordon, Re-examining the chemical evaluation of diagenesis in human bone apatite, J. Archaeol. Sci. 38 (2011) 2222–2230, http://dx.doi.org/10.1016/j.jas.2011.03.023.
- [25] K. Meissner, T. Lippert, A. Wokaun, D. Guenther, Analysis of trace metals in comparison of laser-induced breakdown spectroscopy with LA-ICP-MS, Thin Solid Films 453–454 (2004) 316–322 <a href="http://dx.doi.org/dx.doi.org/0.1016/j.tsf.2003.11">http://dx.doi.org/dx.doi.org/0.1016/j.tsf.2003.11</a>. 1745.
- [26] S.C. Jantzi, J.R. Almirall, Elemental analysis of soils using laser ablation inductively coupled plasma mass spectrometry (LA-ICP-MS) and laser-induced breakdown spectroscopy (LIBS) with multivariate discrimination: tape mounting as an alternative to pellets for small forensic transfer specimens, Appl. Spectrosc. 68 (2014) 963–974, http://dx.doi.org/10.1366/13-07351.
- [27] T. Trejos, A. Flores, J.R. Almirall, Micro-spectrochemical analysis of document paper and gel inks by laser ablation inductively coupled plasma mass spectrometry and laser induced breakdown spectroscopy, Spectrochim. Acta B 65 (2010) 884–895, http://dx.doi.org/10.1016/j.sab.2010.08.004.
- [28] M. Galiová, J. Kaiser, F.J. Fortes, K. Novotný, R. Malina, L. Prokeš, A. Hrdlička, T. Vaculovič, M. Nývltová Fišáková, J. Svoboda, V. Kanický, J.J. Laserna, Multielemental analysis of prehistoric animal teeth by laser-induced breakdown spectroscopy and laser ablation inductively coupled plasma mass spectrometry, Appl. Opt. 49 (2010) 191–199, http://dx.doi.org/10.1364/AO.49.00C191.
- [29] B.E. Naes, S. Umpierrez, S. Ryland, C. Barnett, J.R. Almirall, A comparison of laser ablation inductively coupled plasma mass spectrometry, micro X-ray fluorescence spectroscopy, and laser induced breakdown spectroscopy for the discrimination of automotive glass, Spectrochim. Acta B 63 (2008) 1145–1150, http://dx.doi.org/10. 1016/i.sab.2008.07.005
- [30] C.M. Bridge, J. Powell, K.L. Steele, M. Williams, J.M. MacInnis, M.E. Sigman, Characterization of automobile float glass with laser-induced breakdown spectroscopy and laser ablation inductively coupled plasma mass spectrometry, Appl. Spectrosc. 60 (2006) 1181–1187, http://dx.doi.org/10.1366/ 000370206778664572.
- [31] K. Subedi, T. Trejos, J. Almirall, Forensic analysis of printing inks using tandem laser induced breakdown spectroscopy and laser ablation inductively coupled plasma mass spectrometry, Spectrochim. Acta B 103–104 (2015) 76–83, http://dx.

- doi.org/10.1016/j.sab.2014.11.011.
- [32] Y. Lee, S. Nam, K. Ham, J. Gonzalez, D. Oropeza, D. Quarles Jr., J. Yoo, R.E. Russo, Multivariate classification of edible salts: simultaneous laser-induced breakdown spectroscopy and laser-ablation inductively coupled plasma mass spectrometry analysis, Spectrochim. Acta B 118 (2016) 102–111, http://dx.doi.org/10.1016/j. sab.2016.02.019.
- [33] N.L. La Haye, M.C. Phillips, A.M. Duffin, G.C. Eiden, S.S. Harilal, The influence of ns- and fs-LA plume local conditions on the performance of a combined LIBS/LA-ICP-MS sensor, J. Anal. At. Spectrom. 31 (2016) 515–522, http://dx.doi.org/10. 1039/C5JA00317B.
- [34] M. Dong, D. Oropeza, J. Chirinos, J.J. González, J. Lu, X. Mao, R.E. Russo, Elemental analysis of coal by tandem laser induced breakdown spectroscopy and laser ablation inductively coupled plasma time of flight mass spectrometry, Spectrochim. Acta B 109 (2015) 44–50, http://dx.doi.org/10.1016/j.sab.2015.04. 008
- [35] C. Latkoczy, T. Ghislain, Simultaneous LIBS and LA-ICP-MS analysis of industrial samples, J. Anal. At. Spectrom. 21 (2006) 1152–1160, http://dx.doi.org/10.1039/ B607697C.
- [36] M. Bonta, J.J. Gonzalez, C.D. Quarles Jr., R.E. Russo, B. Hegedus, A. Limbeck, Elemental mapping of biological samples by the combined use of LIBS and LA-ICP-MS, J. Anal. At. Spectrom. 31 (2016) 252–258, http://dx.doi.org/10.1039/ C51A002876
- [37] J.R. Chirinos, D.D. Oropeza, J.J. Gonzalez, H. Hou, M. Morey, V. Zorba, R.E. Russo, Simultaneous 3-dimensional elemental imaging with LIBS and LA-ICP-MS, J. Anal. At. Spectrom. 29 (2014) 1292–1298, http://dx.doi.org/10.1039/C4JA00066H.
- [38] S. Pages-Camagna, E. Laval, D. Vigears, A. Duran, Non-destructive and in situ analysis of Egyptian wall paintings by X-ray diffraction and X-ray fluorescence portable systems, Appl. Phys. A 100 (2010) 671–681, http://dx.doi.org/10.1007/ s00339-010-5667-3.
- [39] A. Paladini, F. Toschi, F. Colosi, G. Rubino, P. Santoro, Stratigraphic investigation of wall painting fragments from Roman villas of the Sabina area, Appl. Phys. A 118 (2015) 131–138, http://dx.doi.org/10.1007/s00339-014-8815-3.
- [40] A. Staicu, I. Apostol, A. Pascu, I. Iordache, V. Damian, M.L. Pascu, Laser induced breakdown spectroscopy stratigraphic characterization of multilayered painted surfaces, Spectrochim. Acta B 74–75 (2012) 151–155, http://dx.doi.org/10.1016/j. sab.2012.06.022.
- [41] O. Syta, K. Rozum, M. Choińska, D. Zielińska, Z. Żukowska, A. Kijowska, B. Wagner, Analytical procedure for characterization of medieval wall-paintings by X-ray fluorescence spectrometry, laser ablation inductively coupled plasma mass spectrometry and Raman spectroscopy, Spectrochim. Acta B 101 (2014) 140–148, http://dx.doi.org/10.1016/j.sab.2014.08.003.
- [42] A.P. Laurie, The identification of pigments used in painting at different periods, with a brief account of other methods of examining pictures, Analyst 55 (1930) 162–179. http://dx.doi.org/10.1039/AN9305500162.
- [43] A. Lo Giudice, A. Re, L. Giuntini, M. Massi, P. Olivero, G. Pratesi, M. Albonico, E. Conz, Multitechnique characterization of lapis lazuli for provenance study, Anal. Bioanal. Chem. 395 (2009) 2211–2217, http://dx.doi.org/10.1007/s00216-009-3039-7
- [44] A. Re, A. Lo Giudice, D. Angelici, S. Calusi, L. Giuntini, M. Massi, G. Pratesi, Lapis lazuli provenance study by means of micro-PIXE, Nucl. Instrum. Methods Phys. Res. Sect. B 269 (2011) 2373, http://dx.doi.org/10.1016/j.nimb.2011.02.070 (237).